Spin-orbit interaction driven dimerization in one dimensional frustrated magnets

Shang-Shun Zhang[1], Nitin Kaushal[1], Elbio Dagotto[1,2], and Cristian D. Batista[1,3]
[1]*Department of Physics and Astronomy, University of Tennessee, Knoxville, Tennessee 37996-1200, USA*
[2]*Materials Science and Technology Division, Oak Ridge National Laboratory, Oak Ridge, Tennessee 37831, USA and*
[3]*Quantum Condensed Matter Division and Shull-Wollan Center, Oak Ridge National Laboratory, Oak Ridge, Tennessee 37831, USA*

We study the effect of spin-orbit interaction on one-dimensional U(1)-invariant frustrated magnets with dominant critical nematic fluctuations. The spin-orbit coupling explicitly breaks the U(1) symmetry of arbitrary global spin rotations about the high-symmetry axis down to Z_2 (invariance under a π-rotation). Given that the nematic order parameter is invariant under a π-rotation, it is relevant to ask if other discrete symmetries can be spontaneously broken. Here we demonstrate that the spin-orbit coupling induces a bond density wave that spontaneously breaks the translational symmetry and opens a gap in the excitation spectrum.

I. INTRODUCTION

Frustrated magnetism is a continuous source of exotic states of matter, [1,2] which challenge the existing characterization probes. Once quantum fluctuations melt the traditional magnetic long-range order, it often happens that the remaining liquid or multipolar orderings do not couple directly to the usual experimental probes. A simple example is provided by the spin nematic phase, which has been proposed as the ground of the one-dimensional (1D) $J_1 - J_2$ Heisenberg model near its saturation field [10–20]. This phase arises from a Bose-Einstein condensation of magnon pairs that appears right below the saturation field $h_{\rm sat}$ [10–14]. The attractive magnon-magnon interaction is generated by a ferromagnetic (FM) nearest neighbor (NN) exchange ($J_1 < 0$), which competes against an antiferromagnetic (AFM) next-nearest-neighbor (NNN) exchange $J_2 > 0$. J_2 must be bigger than $|J_1|/4$ for the zero field ground state not to be ferromagnetic.

Several quasi-1D materials are indeed described to a good approximation by the $J_1 - J_2$ model with FM and AFM exchange interactions J_1 and J_2, respectively. $Rb_2Cu_2Mo_3O_{12}$ [21,22] and $LiCuVO_4$ [23,25–33] are two examples. However, the experimental observation of the predicted nematic ordering is challenging due to the lack of a direct probe for testing this kind of ordering. Given the symmetry of the order parameter, the nematic spin ordering is expected to induce a local quadrupolar electric moment via the always present spin-orbit coupling. However, a finite spin-orbit coupling has the additional effect of breaking the global U(1) symmetry of spin rotations along the magnetic field axis down to a finite group. For most of the known compounds, this group is not bigger than Z_2 for any direction of the applied magnetic field (only C_2 rotation axes). This fact raises another concern because the nematic order parameter $\langle S^+_r S^+_{r+1}\rangle$ does not break the remaining Z_2 group (it is invariant under π-rotations).

These simple observations imply that if some form of ordering exists right bellow the saturation field of these compounds, it should not be called "nematic ordering" because of the relevant role of the always present spin-orbit coupling. However, we can expect that the dominant nematic susceptibility of the U(1) invariant model may still lead to discrete broken symmetries in the presence of spin-orbit interaction. If this is the case, it is important to identify those discrete symmetries.

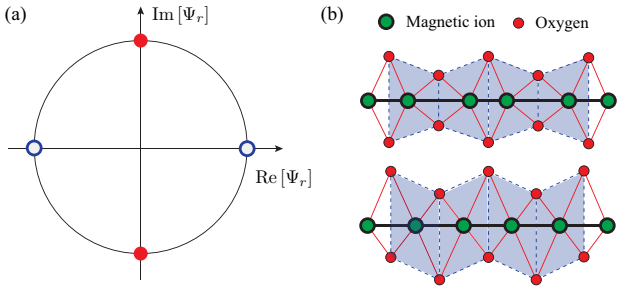

FIG. 1. (Color online) (a) The two scenarios of nematic bond order parameter $\Psi_r = \langle S^+_r S^+_{r+1}\rangle = \langle O^a\rangle + i\langle O^b\rangle$: open and full circles represent the real, $\langle O^a\rangle$, and imaginary, $\langle O^b\rangle$ parts of the nematic order parameter, respectively. (b) Lattice distortions induced via spin-orbit coupling by the real (upper panel) and the imaginary (lower panel) parts of the bond nematic order parameter. Translational symmetry is broken in both cases, but the lattice distortion takes place along different directions. The bigger circles represent the magnetic transition-metal ions. The smaller circles represent the oxygen atoms that mediate the super-exchange interaction.

In this work we investigate the relevant effect of spin-orbit interaction on the 1D frustrated $J_1 - J_2$ model. Based on our previous considerations, there are two possible scenarios: i) The field-induced transition from a quantum paramagnet to the nematic phase is replaced by a crossover (no discrete symmetry breaking); ii) The field-induced transition from a quantum paramagnet to the nematic phase is replaced by a discrete symmetry breaking. We can anticipate that the problem under consideration belongs to the second case because it is known that the magnon-pairs condense at a finite wave vector $\pm Q$. In other words, the nematic ordering breaks the translational symmetry, which is not affected by the inclusion of the spin-orbit interaction. The system has another Z_2 symmetry besides the π-rotation about the z-axis. This symmetry is the product of two operations, $\mathcal{T}\mathcal{R}(\pi)$, where $\mathcal{T}$ is the time reversal operator and $\mathcal{R}(\pi)$ is a π-rotation operator about an axis perpendicular to the field direction. We will find that the real part of the nematic order parameter, O^a, preserves this Z_2 symmetry, while the imaginary part, O^b, does not. Therefore, stabilization of the real or imaginary part of the neamatic order parameter leads to the different broken symmetry states illustrated in Fig. 1 (a).

In the following sections, we derive a phenomenological Ginzburg-Landau theory that is complemented by microscopic analytical and numerical calculations. Moreover, we demonstrate that the combined effect of a divergent nematic susceptibility and a finite spin-orbital coupling leads to a bond ordering, which corresponds to simple bond dimerization for most of the phase diagram. This bond ordering is accompanied by an orthorhombic distortion of the surrounding oxygen octahedron, as it is schematically shown in the upper panel of Fig. 1 (b). In contrast, the phase associated with an imaginary "nematic" order parameter, O^b, does not produce bond dimerization. In addition, this phase becomes unstable upon inclusion of the spin orbit interaction. If stabilized by other mechanisms, this phase would produce a local orthorhombic distortion of the surrounding oxygen octahedron along diagonal directions, as illustrated in the lower panel of Fig. 1 (b).

Given that bond dimerization couples to the lattice via magneto-elastic interaction and lowers the space group of the material under consideration, this combined effect of high spin-nematic susceptibility and a finite spin-orbit coupling could be detected with X-rays. In addition, the incommensurate bond-density wave that is expected for smaller values of $J_2/|J_1|$ should lead to a double-horn shape of the nuclear magnetic resonance (NMR) line. These conclusions can shed light on the search for the spin "nematic ordering" predicted on the basis of a U(1) invariant $J_1 - J_2$ Heisenberg model.

The structure of this paper is as follows: In Sec. II, we introduce a simple model Hamiltonian in which the U(1) symmetry is reduced to Z_2 via the inclusion of an Ising term (symmetric anisotropy). In Sec. III we consider a simple Ginzburg-Landau (GL) theory, which describes the possible scenarios that can be expected for this model. The phenomenological input parameters of the GL theory are calculated in Sec. IV by means of an analytical approach to the microscopic Hamiltonian. The results of this analytical approach are confirmed by numerical Density Matrix Renormalization Group (DMRG) calculations presented in Sec. V. The general implications of our results for experimental studies of unconventional magnetic ordering in quasi-1D frustrated compounds are discussed in Sec. VI.

II. MODEL HAMILTONIAN

We consider a spin-1/2 anisotropic Heisenberg model on a 1D chain with ferromagnetic nearest-neighbor exchange, $J_1 < 0$, and antiferromagnetic next nearest neighbor exchange $J_2 > 0$:

$$\mathcal{H} = J_1 \sum_j \mathbf{S}_j \cdot \mathbf{S}_{j+1} + J_2 \sum_j \mathbf{S}_j \cdot \mathbf{S}_{j+2} - h \sum_j S^z_j + \alpha \sum_j S^x_j S^x_{j+1}, \quad (1)$$

The last term is an Ising interaction, which arises from the spin-orbit coupling and reduces the U(1) symmetry of continuous spin rotations along the field axis to Z_2[34]. We note that the U(1) symmetry is restored in this model if the magnetic field is applied along the x-direction. In real quasi-1D materials, however, the U(1) symmetry is not present for any direction of the magnetic field because of the presence of other chains. In spite of these considerations, the U(1) invariant model has been invoked to describe various quasi-1D transition metal compounds.

Based on the U(1) invariant model ($\alpha = 0$), several authors proposed that nematic quasi-long range ordering should be observed right below the saturation field $h_{\rm sat}$[10–14]. $h_{\rm sat}$ is finite only for $J_2 > |J_1|/4$ because the zero field ground state is ferromagnetic for $J_2 \leq |J_1|/4$. The nematic ordering corresponds to a Bose-Einstein condensation of two-magnon bound states with a local order parameter $\langle S^+_j S^+_{j+1}\rangle$. The attractive magnon-magnon interaction is provided by the ferromagnetic nearest-neighbor exchange J_1. The ratio $\rho = J_2/|J_1|$ controls the total momentum $\pm Q$ of the two-magnon bound state. Q is incommensurate for small values of ρ and it is equal to π for $\rho \geq 0.379$.

In general, the continuous SU(2) symmetry of the Heisenberg interaction is broken down to a discrete symmetry group in real materials[22,23]. Even for an idealized single-chain system, the exchange interaction turns out to be anisotropic, instead of SU(2) invariant, once the spin-orbit interaction is included. This is so because an isolated chain has only one symmetry axis parallel to the chain direction (x-direction in our notation). In other words, the exchange interaction between spin components parallel to the chain direction is different from the exchange interaction between the spin components perpendicular to the chain direction, as it is clear from the α-term in Eq. (1). Consequently, the pure 1D Hamiltonian has only discrete point group symmetries if the external magnetic field is not parallel to the chain direction. For the case under consideration (magnetic field perpendicular to the chain direction), the U(1) symmetry of the Heisenberg model is reduced to a discrete Z_2 symmetry corresponding to a π-rotation about the z-axis $\mathcal{R}_z(\pi):\ S^z_r \to S^z_r, S^{x,y}_r \to -S^{x,y}_r$. Correspondingly, the spin components $S^\pm_r$ transform into $e^{\pm i\phi} S^\pm_r$ under a rotation by ϕ about the z-axis. This means that the nematic order parameter, $\langle S^+_r S^+_r\rangle$, transforms into $e^{i2\phi}\langle S^+_r S^+_r\rangle$, implying that it is invariant under π-rotations, as expected for a director. Consequently, the inclusion of a finite spin-orbit coupling forces us to rethink the whole problem because other symmetries (different from rotations) have to be invoked to characterize the phase that replaces the nematic quasi-long range ordering.

Besides the above mentioned π rotation about the z-axis, the Hamiltonian of Eq. (1) is invariant under the product of the time reversal operation and a π-rotation about the y-axis, $\mathcal{T}\mathcal{R}_y(\pi)$, which changes the sign of the x and z spin components: $S^{x,z}_r \to S^{x,z}_r, S^y_r \to -S^y_r$. The real-part of the nematic order parameter,

$$\Re\langle S^+_r S^+_{r+1}\rangle = \langle S^x_r S^x_{r+1} - S^y_r S^y_{r+1}\rangle \equiv \langle O^a(r)\rangle, \quad (2)$$

remains invariant under this transformation. In contrast, the imaginary part,

$$\Im\langle S^+_r S^+_{r+1}\rangle = \langle S^x_r S^y_{r+1} + S^y_r S^x_{r+1}\rangle, \quad (3)$$

changes sign. Finally, the nematic order parameter breaks the translational symmetry because, as we already mentioned, the magnon-pairs condense at a finite momentum $\pm Q$. This symmetry is then expected to break spontaneously for $\alpha \neq 0$, as long as Q is commensurate.

Based on this simple symmetry analysis, we expect that the finite spin-orbit coupling should stabilize a state that breaks the translational symmetry (in a strong or a weak sense) and selects either the real or the imaginary part of the original nematic order parameter. Only one of these two components should be selected, as supposed to some linear combination, because they belong to different irreducible representations of the point group of $\mathcal{H}$.

III. GINZBURG-LANDAU THEORY

The attractive interaction between magnons arising from the ferromagnetic nearest-neighbor interaction, leads to two-magnon bound states for $J_2/|J_1| > 1/4$. The minimum energy of the two-magnon bound state is achieved for a finite value, $\pm Q$, of the center of mass momentum. The two-magnon bound states condense for $h < h_c$ (note that h_c is higher than the field required to close the single-magnon gap). The two-magnon condensate is characterized by a two component complex order parameter $\Psi_{\pm Q}$ (macroscopic wave function of condensate) whenever $Q \neq -Q$. The spin-orbit interaction generates an effective coupling between these two components, as it can be inferred from the lowest order expansion of the Ginzburg-Landau free energy:

$$\mathcal{F} = r\left(|\Psi_Q|^2 + |\Psi_{\bar{Q}}|^2\right) + u\left(\Psi_Q^* \Psi_{\bar{Q}}^* + \Psi_{\bar{Q}} \Psi_Q\right), \tag{4}$$

where $\bar{Q} = -Q$. Due to the restriction of Z_2 symmetry, the complex field $\Psi_{\pm Q}$ is fixed up to a phase factor ± 1. We have also assumed u is real based on the underlying microscopic theory. We would first assume $Q = \pi$ which is an invariant momentum under spatial inversion and exists for parameters $J_2 > J_{2c}$ ($J_{2c} \simeq 0.379|J_1|$ for $\alpha = 0$). Under this situation, we have $\Psi_\pi = \Psi_{-\pi}$. Then, upon minimization of the free energy, we obtain a real order parameter Ψ_π for $u < 0$, and a purely imaginary order parameter for $u > 0$. In the original spin language, we have $\Psi_\pi = \frac{1}{N}\sum_r e^{i\pi r}\langle S_r^- S_{r+1}^-\rangle$, whose real and imaginary part correspond to

$$\mathcal{O}^a = \sum (-1)^r \langle S_r^x S_{r+1}^x - S_r^y S_{r+1}^y\rangle, \tag{5}$$

$$\mathcal{O}^b = -\sum (-1)^r \langle S_r^x S_{r+1}^y + S_r^y S_{r+1}^x\rangle. \tag{6}$$

A real order parameter only breaks the translational symmetry, while an imaginary order parameter breaks additional symmetries, such as, $\mathcal{TR}_y(\pi)$: $S_r^{x,z} \to S_r^{x,z}, S_r^y \to -S_r^y$. In both cases, the system should develop long-range ordering at $T = 0$ because only discrete symmetries are broken. We note that the spin-orbit interaction leads to a linear coupling to the uniform component $\Psi_0 = \frac{1}{N}\sum_r \langle S_r^- S_{r+1}^-\rangle$, implying that this quantity is finite for a finite spin-orbit coupling. As we will see next, the interference between this uniform component and the π component, Ψ_π, of the *real* order parameter leads to a real space modulation (dimerization) of bond operators.

In general, the nematic order parameter is a complex number, $|\Psi_\pi| e^{i\theta}$, where $\theta = 0$ and $\theta = \frac{\pi}{2}$ correspond to $\mathcal{O}^a$ and $\mathcal{O}^b$, respectively. The real space version of these order parameters is obtained via a Fourier transformation,

$$\mathcal{O}^a(r) = \Psi_0 + 2(-1)^r \Psi_\pi \cos(\theta), \tag{7}$$

$$\mathcal{O}^b(r) = 2(-1)^r \Psi_\pi \sin(\theta), \tag{8}$$

which gives the real and imaginary parts of $\Psi_r = \langle c_r c_{r+1}\rangle$. It is clear that the amplitude of the real component, $\mathcal{O}^a(r)$, is modulated in real space for finite values of the spin-orbit interaction ($\Psi_0 \neq 0$). In contrast, only the phase is modulated for $\alpha = 0$. In other words, the spin-orbit coupling induces a *dimerized bond ordering* if the real component of the original nematic order parameter is selected. This interference between the 0 and π components of $\mathcal{O}^a$ also leads to a *magnon pair* density wave:

$$\begin{aligned} n_{pair}(r) &= \langle \Psi_r^\dagger \Psi_r\rangle \simeq \langle \Psi_r\rangle^* \langle \Psi_r\rangle \\ &= \Psi_0^2 + 4\Psi_\pi^2 + 4(-1)^r \Psi_0 \Psi_\pi \cos(\theta). \end{aligned} \tag{9}$$

It follows that the long range $\mathcal{O}^a$ ordering is accompanied by another bond ordering associated with the longitudinal spin component

$$\langle S_r^z S_{r+1}^z\rangle \simeq \langle \Psi_r\rangle^* \langle \Psi_r\rangle + const. \tag{10}$$

This is just the usual bond dimerization that appears in spin-Peierls systems[24]. Indeed, (10) implies that the usual bond order parameter, $\langle \mathbf{S}_r \cdot \mathbf{S}_{r+1}\rangle$, must also exhibit dimerization.

The condensation wave vector becomes incommensurate ($Q < \pi$) for smaller values of $J_2/|J_1|$ (about 0.379 for $\alpha = 0$). In this case we need to consider a two component order parameter with phases $e^{i\theta_\pm}$ for $\pm Q$. Minimization of the free energy leads to $\theta_+ + \theta_- = 0 \bmod (2\pi)$ for $u < 0$ and to $\phi_+ + \phi_- = \pi \bmod (2\pi)$ for $u > 0$. The complex order parameter does not have a fixed phase because of the additional $U(1)$ phase factor $e^{\pm iQr}$, arising from translational symmetry. This $U(1)$ symmetry precludes long-range order for the single-chain problem. The free energy minimization also leads to the same amplitude for both components of the order parameter: $|\Psi_Q| = |\Psi_{\bar{Q}}|$. This implies that the ground state must exhibit quasi-long range bond density wave order $\mathcal{O}^a(r) = \Psi_0 + 2|\Psi_Q| \cos(Qr)$ or $\mathcal{O}^b(r) = 2|\Psi_Q| \sin(Qr)$.

IV. MICROSCOPIC THEORY

Our discussion in the previous section indicates that two different kinds of bond order can be induced by the spin-orbit interaction. To determine which order parameter is selected we need to consider the underlying microscopic theory. The magnon pair condensate can be approximated by a coherent state built with the two-particle wave function of the bound state. In this section, we study the formation of the two-magnon bound state by solving the corresponding Bethe-

Salpeter equation. To this end, we use the Jordan-Wigner transformation to reformulate the spin Hamiltonian (1) as a model for interacting spinless fermions:

$$S_j^+ = e^{-i\pi\sum_{k=1}^{j-1} n_k} c_j^\dagger, \tag{11}$$

$$S_j^- = e^{i\pi\sum_{k=1}^{j-1} n_k} c_j, \tag{12}$$

$$S_j^z = c_j^\dagger c_j - \frac{1}{2}, \tag{13}$$

where c_j is the fermionic spinless operator which represents a spin flip on site j. The fermionic Hamiltonian is defined as

$$\mathcal{H} = \mathcal{H}_0 + \mathcal{H}_{int},$$

where

$$\mathcal{H}_0 = \sum_k c_k^\dagger c_k \left(J_1 \cos k + J_2 \cos 2k - (h + J_1 + J_2)\right) + i\frac{\alpha}{4}\sum_k \sin k \left(c_k^\dagger c_{-k}^\dagger - c_{-k} c_k\right). \tag{14}$$

For $\alpha = 0$, the single-particle spectrum, corresponding to single-magnon excitations, has a minimum at $k_0 = \arccos(-\frac{J_1}{4J_2})$ if $4J_2 > |J_1|$ and at $k_0 = 0$ if $4J_2 < |J_1|$. The spin-orbit interaction ($\alpha \neq 0$) breaks the $U(1)$ symmetry and the fermion number is no longer conserved. The interacting part of the Hamiltonian is

$$\mathcal{H}_{int} = \frac{1}{2N}\sum_{Q,q,p} U(Q,q,p) c^\dagger_{\frac{Q}{2}+p} c^\dagger_{\frac{Q}{2}-p} c_{\frac{Q}{2}-q} c_{\frac{Q}{2}+q}, \tag{15}$$

where

$$U(Q,q,p) = 2(J_1 + 2J_2\cos Q)\sin(q)\sin(p) \tag{16}$$

$$+ 2J_2 \sin(2q)\sin(2p). \tag{17}$$

The effective attractive interaction between nearest neighbor sites, $J_1 + 2J_2\cos Q$, is maximized at $Q = \pi$. Therefore, the lowest energy two-magnon bound state is expected to have this momentum for large enough $J_2/|J_1|$.

A. Bogoliubov representation

The above non-interacting fermionic Hamiltonian can be diagonalized with a Bogoliubov transformation,

$$c_k = \left(u_k \alpha_k + v_k \alpha_{-k}^\dagger\right) e^{i\frac{\pi}{4}}, \tag{18}$$

$$c_k^\dagger = \left(u_k \alpha_k^\dagger + v_k \alpha_{-k}\right) e^{-i\frac{\pi}{4}}, \tag{19}$$

where

$$u_k = \sqrt{\frac{1}{2}\left(1 + \frac{\epsilon_k}{E_k}\right)}, \tag{20}$$

$$v_k = -sign(\Delta_k)\sqrt{\frac{1}{2}\left(1 - \frac{\epsilon_k}{E_k}\right)}, \tag{21}$$

with $E_k = \sqrt{\epsilon_k^2 + 4\Delta_k^2}$, $\Delta_k = \frac{\alpha}{4}\sin k$ and

$$\epsilon_k = J_1\cos k + J_2 \cos 2k - (h + J_1 + J_2). \tag{22}$$

The diagonal Hamiltonian

$$\mathcal{H}_0 = \sum_k E_k \alpha_k^\dagger \alpha_k + E_0. \tag{23}$$

leads to the non-interacting Green's function

$$iG_0(k,\omega) = \langle 0|\mathcal{T}\alpha_k^\dagger \alpha_k|0\rangle = \frac{i}{\omega - E_k + i0^+}. \tag{24}$$

Now, we rewrite the interaction vertex in terms of Bogoliubov particles. The normal interaction term is

$$\mathcal{H}_{int}^N = \frac{1}{4N}\sum_{Q,q,p} \Gamma_Q^{(0)N}(q,p)\alpha^\dagger_{\frac{Q}{2}+p}\alpha^\dagger_{\frac{Q}{2}-p}\alpha_{\frac{Q}{2}-q}\alpha_{\frac{Q}{2}+q}, \tag{25}$$

with a normal interaction vertex

$$\Gamma_Q^{(0)N}(q,p) = 2U(Q,q,p)\times\left(u_{\frac{Q}{2}+p}u_{\frac{Q}{2}-p}u_{\frac{Q}{2}-q}u_{\frac{Q}{2}+q} + v_{\frac{Q}{2}+p}v_{\frac{Q}{2}-p}v_{\frac{Q}{2}-q}v_{\frac{Q}{2}+q}\right) \tag{26}$$

$$- 4U(p+q, \frac{Q-p+q}{2}, \frac{Q+p-q}{2})\left(u_{\frac{Q}{2}+p}v_{\frac{Q}{2}-p}v_{\frac{Q}{2}-q}u_{\frac{Q}{2}+q} + u_{\frac{Q}{2}-p}v_{\frac{Q}{2}+p}v_{\frac{Q}{2}+q}u_{\frac{Q}{2}-q}\right). \tag{27}$$

We can verify that $\Gamma_Q^{(0)N}(q,p) = \Gamma_Q^{(0)N}(-q,-p)$ due to the fermionic statistics. Furthermore, $\Gamma_Q^{(0)N}(q,p) = \Gamma_{\bar{Q}}^{(0)N}(-q,-p) = \Gamma_{\bar{Q}}^{(0)N}(q,p)$ because of inversion symmetry. The interaction vertex has been symmetrized with respect to the exchange of external lines. The anomalous interaction terms of the form $\alpha^\dagger\alpha^\dagger\alpha^\dagger\alpha^\dagger$ and $\alpha\alpha\alpha\alpha$ are

$$\mathcal{H}_{int}^A = \frac{1}{4!N}\sum_{Q,q,p}\Gamma_Q^{(0)A}(q,p)\left(\alpha^\dagger_{\frac{Q}{2}+p}\alpha^\dagger_{\frac{Q}{2}-p}\alpha^\dagger_{-\frac{Q}{2}+q}\alpha^\dagger_{-\frac{Q}{2}-q} + h.c.\right), \tag{28}$$

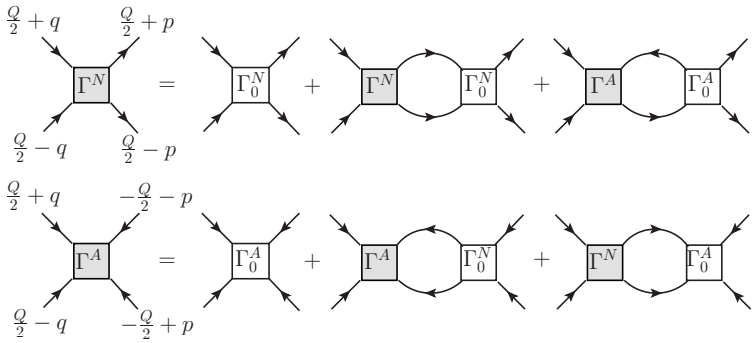

FIG. 2. Ladder diagrams for the normal and anomalous scattering amplitudes Γ^N and Γ^A.

with an anomalous interaction vertex

$$\Gamma_Q^{(0)A}(q,p) = 2U(Q,q,p)\left(u_{\frac{Q}{2}+p}u_{\frac{Q}{2}-p}v_{\frac{Q}{2}-q}v_{\frac{Q}{2}+q} + v_{\frac{Q}{2}+p}v_{\frac{Q}{2}-p}u_{\frac{Q}{2}-q}u_{\frac{Q}{2}+q}\right) \tag{29}$$

$$- 2U(p+q, \frac{Q-p+q}{2}, \frac{Q+p-q}{2})\left(u_{\frac{Q}{2}+p}v_{\frac{Q}{2}-p}u_{\frac{Q}{2}-q}v_{\frac{Q}{2}+q} + v_{\frac{Q}{2}+p}u_{\frac{Q}{2}-p}v_{\frac{Q}{2}-q}u_{\frac{Q}{2}+q}\right) \tag{30}$$

$$+ 2U(p-q, \frac{Q+p+q}{2}, \frac{Q-p-q}{2})\left(v_{\frac{Q}{2}+p}u_{\frac{Q}{2}-p}u_{\frac{Q}{2}-q}v_{\frac{Q}{2}+q} + u_{\frac{Q}{2}+p}v_{\frac{Q}{2}-p}v_{\frac{Q}{2}-q}u_{\frac{Q}{2}+q}\right). \tag{31}$$

We can verify that $\Gamma_Q^{(0)A}(q,p) = \Gamma_{\bar{Q}}^{(0)A}(p,q) = \Gamma_Q^{(0)A}(-q,-p)$ due to fermionic statistics and further more $\Gamma_Q^{(0)A}(q,p) = \Gamma_{\bar{Q}}^{(0)A}(-q,-p) = \Gamma_{\bar{Q}}^{(0)A}(q,p)$ due to inversion symmetry. This interaction vertex has also been symmetrized with respect to the exchange of external lines.

The remaining anomalous terms ($\alpha^\dagger\alpha^\dagger\alpha^\dagger\alpha$ and $\alpha\alpha\alpha\alpha^\dagger$) will not be considered because their contributions are relatively small in the low density limit.

B. Bethe-Salpeter equation

In the dilute limit, the scattering amplitude can be calculated by summing up the ladder diagrams shown in Fig. 2. This sum leads to the Bethe-Salpeter equation:

$$\Gamma_{\omega Q}^N(q,p) = \Gamma_Q^{(0)N}(q,p) - \frac{1}{2N}\sum_k \frac{\Gamma_Q^{(0)N}(Q;q,k)\Gamma_{\omega Q}^N(k,p)}{E_{\frac{Q}{2}+k}+E_{\frac{Q}{2}-k}-\omega-i0^+} - \frac{1}{2N}\sum_k \frac{\Gamma_Q^{(0)A}(q,k)\Gamma_{\omega Q}^A(k,p)}{E_{\frac{Q}{2}+k}+E_{\frac{Q}{2}-k}+\omega-i0^+}, \tag{32}$$

$$\Gamma_{\omega Q}^A(q,p) = \Gamma_Q^{(0)A}(q,p) - \frac{1}{2N}\sum_k \frac{\Gamma_Q^{(0)N}(q,k)\Gamma_{\omega Q}^A(k,p)}{E_{\frac{Q}{2}+k}+E_{\frac{Q}{2}-k}+\omega-i0^+} - \frac{1}{2N}\sum_k \frac{\Gamma_Q^{(0)A}(q,k)\Gamma_{\omega Q}^N(k,p)}{E_{\frac{Q}{2}+k}+E_{\frac{Q}{2}-k}-\omega-i0^+}, \tag{33}$$

where $\Gamma_Q^{(0)N/A}$ is the bare scattering amplitude of the normal and anomalous type. The energy of the magnon pair bound state can be extracted from the poles of the scattering amplitude. For a wide range of $J_2/|J_1|$ values, the bound state dispersion has its minimum at $Q = \pi$. The energy of the two-magnon bound state increases with α, implying that the saturation field decreases relative to the isotropic case.

For the isotropic Heisenberg model, the wave function has a $U(1)$ phase freedom. In the presence of spin-orbit interaction, this freedom is reduced to Z_2. The Ginzburg-Landau theory tells us that the phase of the macroscopic wave function can either be real or imaginary depending on the sign of the effective anomalous coupling parameter u. In this section, we determine the phase of the wave function and also include a microscopic calculation of the parameter u. These properties are enclosed in the scattering amplitude obtained from the Bethe-Salpeter equation. Our analysis indicates that the real space wave wave function of the magnon pair condensate is real, implying that the dominant order parameter is $\mathcal{O}^a$.

1. *Wave function of the bound state*

We start by introducing the two-magnon Green's function, which can be easily obtained through the scattering amplitude

$\Gamma^{N/A}_{\omega Q}(q,p)$:

$$G^{(2)}(\omega,Q;q,p) = G^{(2)}_0(\omega,Q;,q,p) + \frac{1}{4}G^{(2)}_0(\omega,Q;q,q') \times \Gamma^{N}_{\omega Q}(q',p')G^{(2)}_0(\omega,Q;p',p), \quad (34)$$

$$G^{(2)}_A(\omega,Q;q,p) = \frac{1}{4}G^{(2)}_0(-\omega,-Q;-q,-q') \times \Gamma^{A}_{\omega Q}(q',p')G^{(2)}_0(-\omega,-Q;-p',-p), \quad (35)$$

where $G^{(2)}_0$ is the non-interacting two particle Green's function:

$$G^{(2)}_0(\omega,Q;q,q') = \frac{\delta(q-q') - \delta(q+q')}{\omega - E_{\frac{Q}{2}+q} - E_{\frac{Q}{2}-q} + i0^+}. \quad (36)$$

The Lehmann representation shows explicitly that the two particle Green's function has the following singular behavior near the pole of bound state, $\omega \sim \omega_B$:

$$G^{(2)}_N(\omega,Q;q,p) \sim \frac{\psi_Q(p)\psi^*_Q(q)}{\omega - \omega_B + i0^+} + \text{regular terms}, \quad (37)$$

$$G^{(2)}_A(\omega,Q;q,p) \sim \frac{\psi_Q(p)\phi_{-Q}(q)}{\omega - \omega_B + i0^+} + \text{regular terms}, \quad (38)$$

where the regular terms come from higher excited states and $\omega_B > 0$ is the bound state energy relative to the ground state. The bound state wave function is obtained from the residue of the pole,

$$\psi_Q(p) = \langle G|\alpha_{\frac{Q}{2}+p}\alpha_{\frac{Q}{2}-p}|B\rangle_Q, \quad (39)$$

$$\phi^*_{\bar{Q}}(p) = \langle G|\alpha^\dagger_{-\frac{Q}{2}-p}\alpha^\dagger_{-\frac{Q}{2}+p}|B\rangle_Q, \quad (40)$$

where $|B\rangle$ is the ket of the bound state and $|G\rangle$ the ground state. Due to the anomalous interaction arising from the spin-orbit interaction, the bound state wave function is a linear combination of states with different number of particles. The poles of the two particle Green's function given by Eqs. (34) and (35) are obtained after inserting the scattering amplitude, $\Gamma^{N/A}_{\omega Q}(q,p)$, which results from the Bethe-Salpeter equation. According to Eqs. (39) and (40), the bound state wave function is then obtained by extracting the residue near the pole ω_B. For $Q = \pi$, the bound state wave functions, $\psi_\pi(p)$ and $\phi_\pi(p)$, are even under spatial inversion. This result is found to be correct for all $J_2/|J_1|$ ratios and for any value of the bound state energy ω_B, indicating that the broken symmetry state below the saturation field must preserve the spatial inversion symmetry.

As the system approaches the critical field corresponding to the onset of the two-magnon condensate, $\omega_B \to 0$, the normal and the anomalous Green's function become exactly the same (see Fig. 3). Consequently, the particle pair wave function, $\psi_Q(p)$, is exactly the same as the hole pair wave function $\phi^*_{\bar{Q}}(p)$. This is a manifestation of an emergent particle-hole symmetry at zero energy, which sets a constraint on the phase of the bound state wave function. If we think of the condensate state as a coherent state built with the two-body bound state wave function, the phases $\theta_\pm$ for the macroscopic components $\Psi_{\pm Q}$ are given by $\psi_Q(p)$ and $\phi_{\bar{Q}}(p)$, respectively. The relationship $\psi_Q(p) = \phi^*_{\bar{Q}}(p)$ indicates that $\theta_+ + \theta_- = 0$, which leads to a real order parameter $\langle S^+_r S^+_{r+1}\rangle$ in real space.

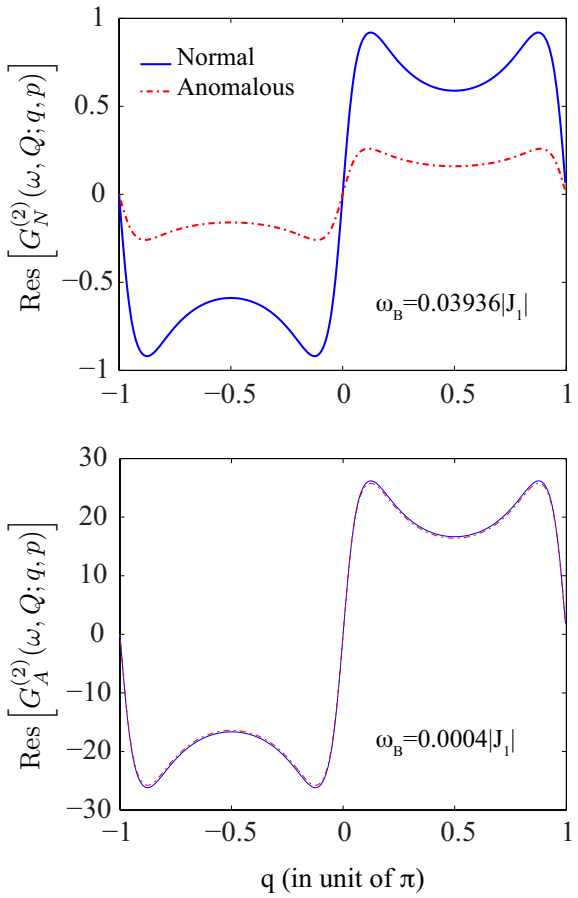

FIG. 3. Residue of the two particle normal/anomalous Green's function near the pole ω_B in frequency space for: (a) $\omega_B/|J_1| = 0.03936$ and (b) $\omega_B/|J_1| = 0.0004$ (close to the two-magnon condensation point). The other parameters are taken as $J_2/|J_1| = 1, \alpha = 0.2$, momentum $p = 0.9\pi$. We find the normal (blue solid line) and anomalous (red dotted line) two-particle Green's function become the same upon approaching the critical condensation point.

Beyond the condensation point, the new ground state, $|G\rangle$, is characterized by the order parameter $\Phi_Q(q) = \langle G|\alpha_{\frac{Q}{2}+q}\alpha_{\frac{Q}{2}-q}|G\rangle$. The coherent representation enables us to identify the bound state wave functions $\psi_Q(p)$ and $\phi_{\bar{Q}}(p)$ with the two component order parameter, $\Phi_Q(p)$ and $\Phi_{\bar{Q}}(p)$, that was discussed in Section III. This correspondence leads to the self-consistent equation for the order parameter based on the Bethe-Salpeter equation, from which one can straightforwardly confirm which order is favored by the system. The analysis becomes more transparent by adopting an equivalent but more straightforward approach. We just introduce a small pairing field term into the Hamiltonian, which couples to the

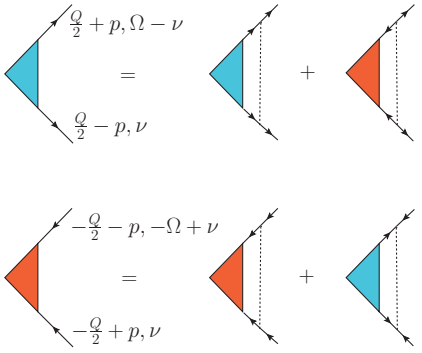

FIG. 4. Ladder diagrams for the pairing field $h^R_{\pm Q}(q)$. The blue (red) vertex represents the renormalized pairing field at Q ($-Q$). The dashed lines represent the symmetrized interaction vertexes in Eqs. (26) and (29).

order parameter:

$$\mathcal{H}_{paring} = h^*_Q \sum_q \alpha_{\frac{Q}{2}+q}\alpha_{\frac{Q}{2}-q} + h^*_{\bar{Q}} \sum_q \alpha_{\frac{Q}{2}+q}\alpha_{\frac{Q}{2}-q} + h.c.. \quad (41)$$

The renormalized pairing fields $h^R_Q, h^R_{\bar{Q}}$ are indicated by the ladder series of vertex corrections in Fig. 4. The pairing susceptibility diverges at the condensation point, implying that the order parameter develops spontaneously beyond this point, i.e., in absence of the pairing fields h_Q and $h_{\bar{Q}}$. The order parameter in momentum space, $\Phi_Q(q) = \langle \alpha_{\frac{Q}{2}+q}\alpha_{\frac{Q}{2}-q}\rangle$, can be calculated as $\Phi_Q(q) = -h^R_Q(q)/\Omega_q$. Therefore, the ladder series of vertex corrections in Fig. 4 leads to the following self-consistent equation:

$$\sum_k \left(\Omega_Q(q)\delta_{q,k} + \frac{1}{2N}\Gamma^{(0)N}_Q(q,k) \pm \Gamma^{(0)A}_Q(k,q)\right)\Phi^{\pm}_Q(k) = 0, \quad (42)$$

where $\Omega_Q(q) = E_{\frac{Q}{2}+q} + E_{\frac{Q}{2}-q}$ is the energy of a two-magnon excitation and

$$\Phi^{\pm}_Q(k) = \Phi_Q(k) \pm \Phi^*_{-Q}(k). \quad (43)$$

The order parameters $\Phi^{\pm}_Q(k)$ become finite when the corresponding matrix in Eq. (42) is singular. For $Q = \pi$, $\Phi^+_\pi(k)$ coincides with imaginary part of $\Phi_\pi(k)$, while $\Phi^-_\pi(k)$ is the real part. The numerical calculation shows that the order parameter $\Phi_\pi(k)$ is purely imaginary for $Q = \pi$ and that it satisfies $\Phi_Q(k) = \Phi^*_{-Q}(k)$ for $Q < \pi$. To understand the meaning of this result in real space, we just need to consider the order parameter $\langle S^-_{r+1}S^-_r\rangle$, which is given by $\langle c_{r+1}c_r\rangle$ in terms of the Jordan-Wigner fermionic annihilation operators. By applying Fourier and Bogoliubov transformations, we find

$$\langle S^-_{r+1}S^-_r\rangle = \Psi_0 - \frac{1}{N}\sum_q u_{\frac{Q}{2}+q}u_{\frac{Q}{2}-q}\sin q \times [\Phi_Q(q)e^{i\frac{Q}{2}}e^{iQr} + \Phi_{\bar{Q}}(q)e^{i\frac{\bar{Q}}{2}}e^{i\bar{Q}r}] - \frac{1}{N}\sum_q v_{\frac{Q}{2}+q}v_{\frac{Q}{2}-q} \times \sin q[\Phi^*_{\bar{Q}}(q)e^{i\frac{Q}{2}}e^{iQr} + \Phi^*_Q(q)e^{i\frac{\bar{Q}}{2}}e^{i\bar{Q}r}]. \quad (44)$$

The relationship $\Phi_Q(q) = \Phi^*_{\bar{Q}}(q)$ implies that the real space order parameter is

$$\langle S^-_{r+1}S^-_r\rangle = \Psi_0 - \frac{2}{N}\sum_q \left(u_{\frac{Q}{2}+q}u_{\frac{Q}{2}-q} + v_{\frac{Q}{2}+q}v_{\frac{Q}{2}-q}\right) |\Phi_Q(q)|\sin q\cos(Qr + Q/2 + \phi_+), \quad (45)$$

where ϕ_+ is the phase angle of $\Phi_Q(q)$. Therefore, the order parameter $\langle S^-_{r+1}S^-_r\rangle$ is real.

2. *Microscopic calculation of phenomenological parameters*

To provide a microscopic derivation of the phenomenological parameters r and u we express the Ginzburg-Landau free energy in its diagonal form:

$$\mathcal{F} = \frac{r+u}{2}|\Psi_+|^2 + \frac{r-u}{2}|\Psi_-|^2, \quad (46)$$

where $\Psi_\pm = \Psi_Q \pm \Psi^*_{\bar{Q}}$ and Ψ_Q is the Fourier transform of the bond order parameter $\langle S^-_r S^-_{r+1}\rangle$. The order parameter can be expressed in terms of the fermionic Bogoliubov quasiparticles,

$$\Psi_\pm = -\frac{e^{iQ/2}}{\sqrt{N}}\sum_q \sin(q)(u_{\frac{Q}{2}+q}u_{\frac{Q}{2}-q} \pm v_{\frac{Q}{2}+q}v_{\frac{Q}{2}-q})\Phi_\pm(q), \quad (47)$$

where $\Phi_\pm(q) = \Phi_Q(q) \pm \Phi^*_{\bar{Q}}(q)$ and $\Phi_Q(q) = \langle \alpha_{\frac{Q}{2}+q}\alpha_{\frac{Q}{2}-q}\rangle$. From Eq. (46), we can identify the phenomenological parameters with the inverse of the corresponding static susceptibilities:

$$r \pm u = \langle(\Psi_\pm)^\dagger\Psi_\pm\rangle^{-1} = (\chi_\pm)^{-1}. \quad (48)$$

In other words, $\chi_\pm$ are the response functions to pairing fields that couple linearly to the $\Psi_\pm$ order parameters given in Eq. (47):

$$\chi_\pm = -\frac{2}{N}\sum_{qp}\frac{\sin q\sin p B^\pm_q B^\pm_p}{\Omega_Q(q)\Omega_Q(p)}\left(\Gamma^N_{0Q}(q,p) \pm \Gamma^A_{0Q}(q,p)\right) + \frac{2}{N}\sum_q \frac{\sin^2 q (B^\pm_q)^2}{\Omega_Q(q)}, \quad (49)$$

where $\Gamma^{N/A}_{0Q}(q,p)$ is the scattering amplitude at zero frequency, $\Omega_Q(q) = E_{\frac{Q}{2}+q} + E_{\frac{Q}{2}-q}$ and $B^\pm_q = u_{\frac{Q}{2}+q}u_{\frac{Q}{2}-q} \pm v_{\frac{Q}{2}+q}v_{\frac{Q}{2}-q}$. The second term is the non-interacting susceptibility of the

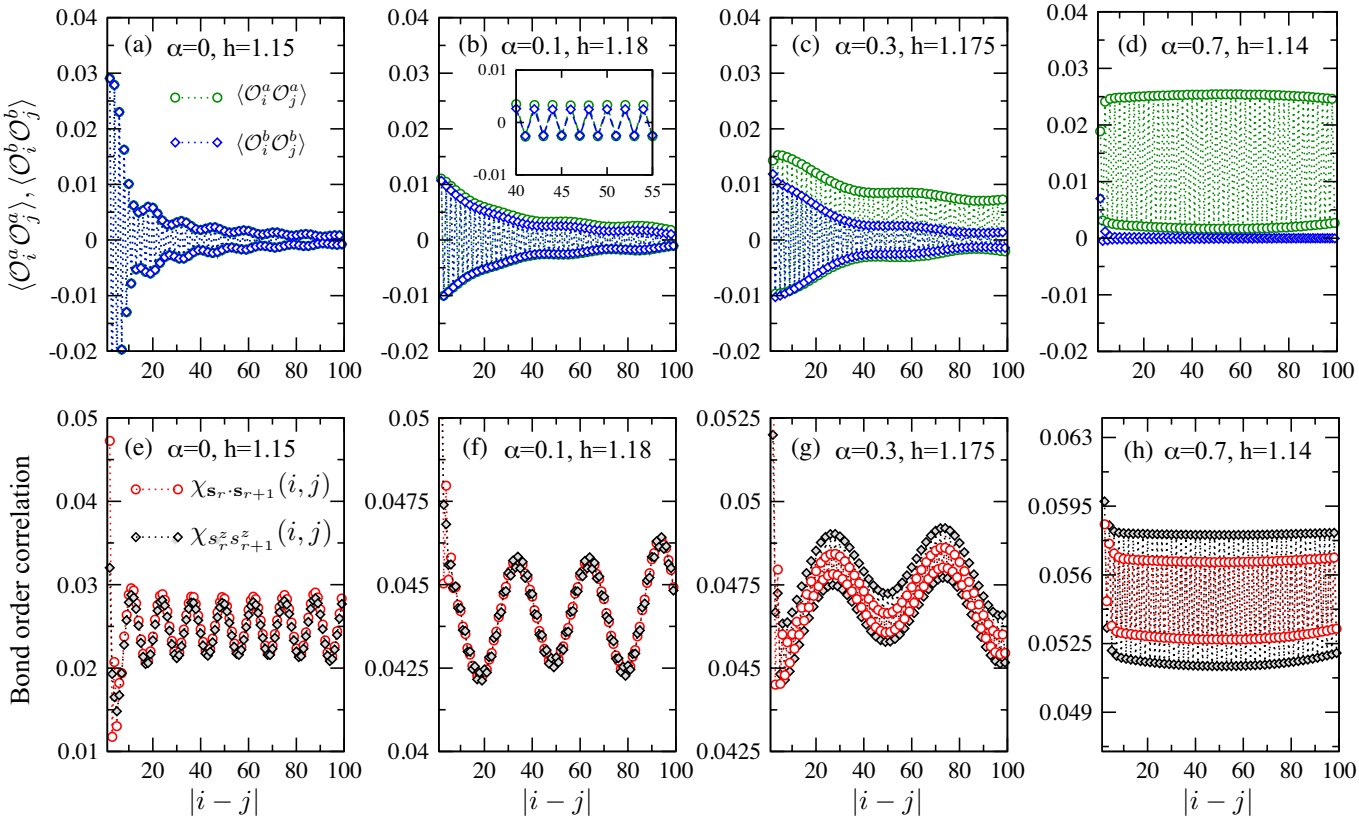

FIG. 5. (Color online) DMRG simulation for a spin chain of length $L = 160$ with open boundary condition. The measurement is made in the bulk with $i = 30$ and $31 < j \leq 130$. (a)-(d) show the correlation function of two types of bond order for different values of α. (e)-(h) show the correlation function of the bond orders $\chi_{\mathbf{S}_r \cdot \mathbf{S}_{r+1}}(i,j) = \langle \mathbf{S}_i \cdot \mathbf{S}_{i+1} \mathbf{S}_j \cdot \mathbf{S}_{j+1} \rangle$ and $\chi_{S_r^z S_{r+1}^z}(i,j) = \langle S_i^z S_{i+1}^z S_j^z S_{j+1}^z \rangle$. The frustration ratio is $J_2/|J_1| = 0.9659$ and the magnetic field is close to the saturation field for each α.

Bogoliubov fermions, which is negligible near the critical point where both $\Gamma_{0Q}^N(q,p)$ and $\Gamma_{0Q}^A(q,p)$ diverge. The finite u value arises from the non-zero anomalous scattering amplitude, $\Gamma_{0Q}^A(q,p)$, which makes the two susceptibilities $\chi_Q^{\pm}$ to be different:

$$u = \frac{\left(\chi_Q^+\right)^{-1} - \left(\chi_Q^-\right)^{-1}}{2}. \tag{50}$$

Numerically, we always find $u < 0$ for different ratios of J_2/J_1, in agreement with our previous discussions.

V. NUMERICAL SIMULATIONS

In this section we present DMRG calculations[36,37] for the anisotropic 1D spin Hamiltonian $\mathcal{H}$, which confirm the analysis presented in the previous sections. All the calculations have been done right below the saturation field for chains of $L = 160$ spins with open boundary conditions. We used up to 400 states and kept truncation tolerance below 10^{-8} throughout the DMRG iterations, and we did 6 full sweeps of finite algorithm of DMRG to get the well converged Ground state and observables. Fig. 5 shows the correlation functions for the real and imaginary parts of the nematic order parameter, $\mathcal{O}^a$, $\mathcal{O}^b$, for the "pair-density" operator $S_i^z S_{i+1}^z$, and for the bond operators $\mathbf{S}_i \cdot \mathbf{S}_{i+1}$, for different values of α. The frustration ratio is taken as $J_2/J_1 = 0.9659$, which gives rise to a lowest energy two-magnon bound state with center of mass momentum equal to π. In agreement with the two-magnon calculation, the correlation functions of the order parameters $\mathcal{O}^a$ and $\mathcal{O}^b$ oscillate with wave vector π. The long wave length oscillations are just a consequence of the open boundary conditions and the large spin density wave susceptibility. Note, however, that the incommensurate nature of oscillations precludes the possibility of having long range spin density wave ordering (the incommensurate spin density wave ordering breaks the continuous U(1) symmetry group of translations).

The first column in Fig. 5 with $\alpha = 0$ corresponds to the U(1) symmetric case for which all the correlators exhibit the expected power law behavior. The order parameters $\mathcal{O}^a$ and $\mathcal{O}^b$ are connected by a $\pi/4$ spin rotation about the z-axis, which is a symmetry of the Hamiltonian for $\alpha = 0$. Correspondingly, both correlation functions exhibit an identical power-law decay. The bond and the pair density correlators also exhibit a power law decay with long wave length oscillations, which are magnified by the open boundary conditions[4].

The upper panels of Fig. 5 show that the real component of the nematic order parameter dominates over the imaginary part and develops long range ordering for nonzero α. As ex-

pected from the previous analysis, the pair density, $S^z_i S^z_{i+1}$, and the bond, $\mathbf{S}_i \cdot \mathbf{S}_{i+1}$, operators become dimerized as a consequence of the coexistence of uniform and staggered components of the O^a order parameter. We recall that the uniform component is directly induced by the α term of the Hamiltonian, while the staggered (π) component is spontaneously generated. It is clear from the figure that the three order parameters become more robust upon increasing α. Another salient feature is that the two-magnon condensate becomes stabilized over a larger window of magnetic field values. Moreover, the Friedel oscillations of $\langle S^z_i \rangle$ are strongly suppressed for $\alpha = 0.7$ and the amplitudes of the three order parameters become significantly larger.

VI. DISCUSSION AND SUMMARY

The quasi-1D compound $LiCuVO_4$ has a anisotropy approximately $\alpha = 0.1$[23,25,28,35]. From our simulation shown by Fig. 5 (b), (f), the bond order correlation develops a visible π ordering. By making a Fourier transformation into the momentum space, we find a finite spectral weight at $Q \simeq \pi$. This provides a salient experimental signature that can be detected with X-rays. $Rb_2Cu_2Mo_3O_{12}$ is another quasi-1D J_1-J_2 frustrated magnet[21,22] with $J_2/|J_1| \simeq 0.33$. This value falls in the region where higher multipolar orderings (quasi-condensate of bound states of more than two magnons) are expected for the U(1) invariant model. Indeed, for $J_2/|J_1| < 0.37$, just bellow the transition point $J_{2c}/|J_1| \simeq 0.379$ between the commensurate and incommensurate nematic phases, the ground state of the U(1) invariant model becomes a quasi-condensate of three-magnon bound states[4,11]. Although we have not considered this situation in the present manuscript, we note that the α-term in the Hamiltonian should once again select the real or the imaginary part of the multipolar order parameter.

In summary, we have demonstrated that the spin-orbit interaction has important consequences for the field-induced spin nematic ordering of U(1) invariant frustrated models. The symmetry reduction of $\mathcal{H}$ due to the presence of the Ising term renders the nematic order parameter inapplicable. However, the real and imaginary parts of the nematic bond order parameter still break discrete symmetries, which can be directly related with rather simple observable quantities. Our analytical and numerical results demonstrate that the spin-orbit interaction stabilizes a bond density wave (bond dimerization for $Q = \pi$) which couples to the lattice via the magneto-elastic interaction. These results are confirmed by our DMRG simulations. Given that the spin-orbit interaction is ubiquitous in nature and that continuous symmetries do not exist in real magnets, our study indicates that the proposed nematic ordering is likely to be replaced by bond dimerization in systems described by a J_1-J_2 model with $|J_2|/|J_1| \gtrsim 0.38$. Even in quasi-1D systems described by a U(1) invariant XXZ model to a good approximation, the application of a magnetic field *perpendicular* to the chains should induce the dimerized state that we are proposing here.

ACKNOWLEDGMENTS

We thank Zhentao Wang, Shi-Zeng Lin and Yukitoshi Motome for helpful discussions. N. K. was supported by the National Science Foundation, under Grant No. DMR-1404375. E. D. was supported by the U.S. Department of Energy, Office of Basic Energy Sciences, Materials Sciences and Engineering Division.

[1] Vivien Zapf, Marcelo Jaime, and C. D. Batista, Rev. Mod. Phys. **86**, 563 (2014).
[2] L. Balents, Nature **464**, 199 (2010).
[3] A. V. Chubukov and O. A. Starykh, Phys. Rev. Lett. **110**, 217210 (2013).
[4] Toshiya Hikihara, Lars Kecke, Tsutomu Momoi, and Akira Furusaki, Phys. Rev. B **78**, 144404 (2008).
[5] Gia-Wei Chern, C. J. Fennie, and O. Tchernyshyov, Phys. Rev. B **74**, 060405 (R) (2006).
[6] P. W. Anderson, Mater. Res. Bull., **8**, 153 (1973).
[7] Fradkin E., *Field Theories of Condensed Matter Systems* (Addison-Wesley, Reading) 1991.
[8] F. L. Pratt, P. J. Baker, S. J. Blundell, T. Lancaster, S. Ohira-Kawamura, C. Baines, Y. Shimizu, K. Kanoda, I. Watanabe, and G. Saito, Nature. **471**, 612 (2011).
[9] X. G. Wen, F. Wilczek, and A. Zee, Phys. Rev. B **39**, 11413 (1989).
[10] M. E. Zhitomirsky and H. Tsunetsugu, Europhys. Lett., **92**, 37001 (2010).
[11] L. Kecke, T. Momoi, and A. Kurusaki, Phys. Rev. B **76**, 060407 (2007).
[12] T. Hikihara, L. Kecke, T. Momoi, and A Furusaki, Phys. Rev. B **78**, 144404 (2008).
[13] A. V. Chubukov, Phys. Rev. B **44**, 4693 (1991).
[14] J. Sudan, A. Lüscher, and A. M. Läuchli, Phys. Rev. B **80**, 140402(R) (2009).
[15] A. Läuchli, J. C. Domenge, C. Lhuillier, P. Sindzingre, and M. Troyer, Phys. Rev. Lett. **95**, 137206 (2005).
[16] Nic Shannon, Tsutomu Momoi, and Philippe Sindzingre, Phys. Rev. Lett. **96**, 027213 (2006).
[17] G. Marmorini and T. Momoi, Phys. Rev. B **89**, 134425 (2014).
[18] Ryuichi Shindou and Tsutomu Momoi, Phys. Rev. B **80**, 064410 (2009).
[19] H. T. Ueda and T. Momoi, Phys. Rev. B **87**, 144417 (2013).
[20] Emika Takata, Tsutomu Momoi, and Masaki Oshikawa, arXiv: 1510.02373.
[21] M. Hase, H. Kuroe, K. Ozawa, O. Suzuki, H. Kitazawa, G. Kido, and T. Sekine, Phys. Rev. B 70, 104426 2004 .
[22] Y. Yasui, R. Okazaki, I. Terasaki, M. Hase, M. Hagihala, T. Masuda, and T. Sakakibara, JPS Conf. Proc. **3**, 014014 (2014)
[23] M. Enderle, C. Mukherjee, B. Fák, R. K. Kremer, J.-M. Broto, H. Rosner, S.-L. Drechsler, J. Richter, J. Malek, A. Prokofiev, W. Assmus, S. Pujol, J.-L. Raggazzoni, H. Rakoto, M. Rheinstädter and H. M. Rønnow, Europhys. Lett., **70** (2), 237 (2005).
[24] J. S. Miller (Ed.): Extended Linear Chain Compounds. Plenum Press, New York and London 1982.

[25] H.-A. K. Nidda, L. E. Svistov, M. V. Eremin, R. M. Eremina, A. Loidl, V. Kataev, A. Validov, A. Prokofiev, and W. Aßmus, Phys. Rev. B **65**, 134445 (2002).
[26] N. Büttgen, W. Kraetschmer, L. E. Svistov, L. A. Prozorova, and A. Prokofiev, Phys. Rev. B **81**, 052403 (2010).
[27] N. Büttgen, H.-A. Krug von Nidda, Phys. Rev. B **81**, 052403 (2010).
[28] N. Büttgen, H.-A. Krug von Nidda, L. E. Svistov, L. A. Prozorova, A. Prokofiev, and W. Aßmus, Phys. Rev. B **76**, 014440 (2007).
[29] F. Schrettle, S. Krohns, P. Lunkenheimer, J. Hemberger, N. Büttgen, H.-A. Krug von Nidda, A. V. Prokofiev, and A. Loidl, Phys. Rev. B **77**, 144101 (2008).
[30] M. G. Banks, F. Heidrich-Meisner, A. Honecker, H. Rakoto, J.-M. Broto and R. K. Kremer, J. Phys.: Condens. Matter **19** 145227 (2007).
[31] B.J. Gibson, R.K. Kremer, A.V. Prokofiev, W. Assmus, G.J. McIntyre, Physica B **350** e253 (2004).
[32] K. Nawa, Y. Okamoto, A. Matsuo, K. Kindo, Y. Kitahara, S. Yoshida, S. Ikeda, S. Hara, T. Sakurai, S. Okubo, H. Ohta, H. Ohta, and Z. Hiroi, J. Phys. Soc. Jpn. **83**, 103702 (2014).
[33] K. Nawa, T. Yajima, Y. Okamoto, and Z. Hiroi, Inorg. Chem. **54**, 5566 (2015).
[34] G. Jackeli and G. Khaliullin, Phys. Rev. Lett. **102**, 017205 (2009).
[35] L. E. Svistov, T. Fujita, H. Yamaguchi, S. Kimura, K. Omura, A. Prokofiev, A. I. Smirnov, Z. Honda and M. Hagiwara, Jetp Lett. **93** 21 (2011).
[36] S. R. White, Phys. Rev. Lett. **69**, 2863 (1992).
[37] S. R. White, Phys. Rev. B **48**, 10345 (1993).